PROTEINS: Structure, Function, and Genetics 45:107–116 (2001)

Molecular Mapping of Thrombin-Receptor Interactions

Youhna M. Ayala, Angelene M. Cantwell, Thierry Rose, Leslie A. Bush, Daniele Arosio, and Enrico Di Cera*
Department of Biochemistry and Molecular Biophysics, Washington University School of Medicine, St. Louis, Missouri

ABSTRACT **In addition to its procoagulant and anticoagulant roles in the blood coagulation cascade, thrombin works as a signaling molecule when it interacts with the G-protein coupled receptors PAR1, PAR3, and PAR4. We have mapped the thrombin epitopes responsible for these interactions using enzymatic assays and Ala scanning mutagenesis. The epitopes overlap considerably, and are almost identical to those of fibrinogen and fibrin, but a few unanticipated differences are uncovered that help explain the higher (90-fold) specificity of PAR1 relative to PAR3 and PAR4. The most critical residues for the interaction with the PARs are located around the active site where mutations affect recognition in the order PAR4 > PAR3 > PAR1. Other important residues for PAR binding cluster in a small area of exosite I where mutations affect recognition in the order PAR1 > PAR3 > PAR4. Owing to this hierarchy of effects, the mutation W215A selectively compromises PAR4 cleavage, whereas the mutation R67A abrogates the higher specificity of PAR1 relative to PAR3 and PAR4. 3D models of thrombin complexed with PAR1, PAR3, and PAR4 are constructed and account for the perturbations documented by the mutagenesis studies. Proteins 2001;45:107–116.** © 2001 Wiley-Liss, Inc.

Key words: thrombin; thrombin receptors; Ala scanning mutagenesis; molecular modeling

INTRODUCTION

The procoagulant function of the serine protease thrombin primarily involves the conversion of fibrinogen into an insoluble fibrin clot.[1] In addition, thrombin promotes platelet aggregation in humans via the proteolytic activation of G-protein coupled receptors PAR1[2,3] and PAR4.[4,5] A third receptor, PAR3, functions in mouse platelets as a cofactor of PAR4 activation,[6] whereas in humans is present in a variety of tissues other than platelets.[7]

Identification of the molecular mechanisms and structural determinants mediating thrombin–receptor interactions is critical for understanding hemostasis and thrombosis. The interaction of thrombin with its receptors has been investigated in great detail especially with regard to the cellular consequences of receptor signaling.[6,8] In contrast, the kinetics of receptor activation and the structural determinants of recognition are understood in considerably less detail. Recent studies have suggested a higher specificity of thrombin in activating PAR1[9] relative to PAR4.[10] Other studies have shown that the integrity of thrombin exosite I[3] and the aryl binding site[9] are important for PAR1 recognition. The crystal structure of thrombin complexed with a fragment of PAR1[11] suggests that PAR1 interacts with thrombin in a manner similar to that of the natural inhibitor hirudin.[12] In this structure, the PAR1 fragment is bound to two distinct thrombin molecules in the unit cell, bridging the active site of one molecule and exosite I of another molecule. As a result of this crystal packing, the sequence $L^{38}DPR^{41}$ of PAR1 occupies the active site of one thrombin molecule in an unusual nonproductive orientation, whereas the distal sequence $K^{51}YEPF^{55}$ makes contacts with residues of exosite I of a second thrombin molecule mimicking the acidic C-terminal tail of hirudin. Ala scanning and deletion mutagenesis of the acidic fragment $K^{51}YEPFWE^{57}$ of PAR1 has revealed the necessity of this sequence in thrombin recognition and singled out residues Y52 and E53 as being important for binding.[3] The crystal structure supports an important role for Y52, but not for E53.[11]

Unambiguous information on thrombin residues involved in the recognition of the PARs requires a systematic mutagenesis study of the enzyme linked to a quantitative assessment of the kinetics of receptor cleavage. These studies are also necessary to validate the conclusions drawn from mutagenesis studies of PAR1[3] and the current crystallographic information on the thrombin–PAR1 complex.[11] In addition, they serve as an important database for understanding the interaction of thrombin with PAR3 and PAR4 on which kinetic, mutagenesis, and structural information is limited. Finally, a mutagenesis study of thrombin residues involved in PAR recognition can identify the binding epitopes for each receptor, and determine whether they are unique amongst the PARs and other procoagulant substrates like fibrinogen and fibrin.

This study is intended to fill a structure-function gap in our current knowledge of thrombin–receptor interactions. Here we examine the kinetics of thrombin interaction with the PARs, extending a strategy recently introduced for the study of thrombin–PAR1 interaction.[9] A number of thrombin mutants, mostly Ala substitutions of solvent-accessible

Abbreviations: FpA, fibrinopeptide A; FpB, fibrinopeptide B; FPR, H-D-Phe-Pro-Arg-p-nitroanilide; PAR1, protease activated receptor 1; PAR3, protease activated receptor 3; PAR4, protease activated receptor 4; PEG, poly(ethylene glycol); Tris, tris(hydroxymethyl)aminomethane.

Grant sponsor: NIH; Grant numbers: HL49413, HL58141.

*Correspondence to: Enrico Di Cera, Department of Biochemistry and Molecular Biophysics, Washington University School of Medicine, Box 8231, St. Louis, MO 63110. E-mail: enrico@biochem.wustl.edu.

Received 1 February 2001; Accepted 12 June 2001

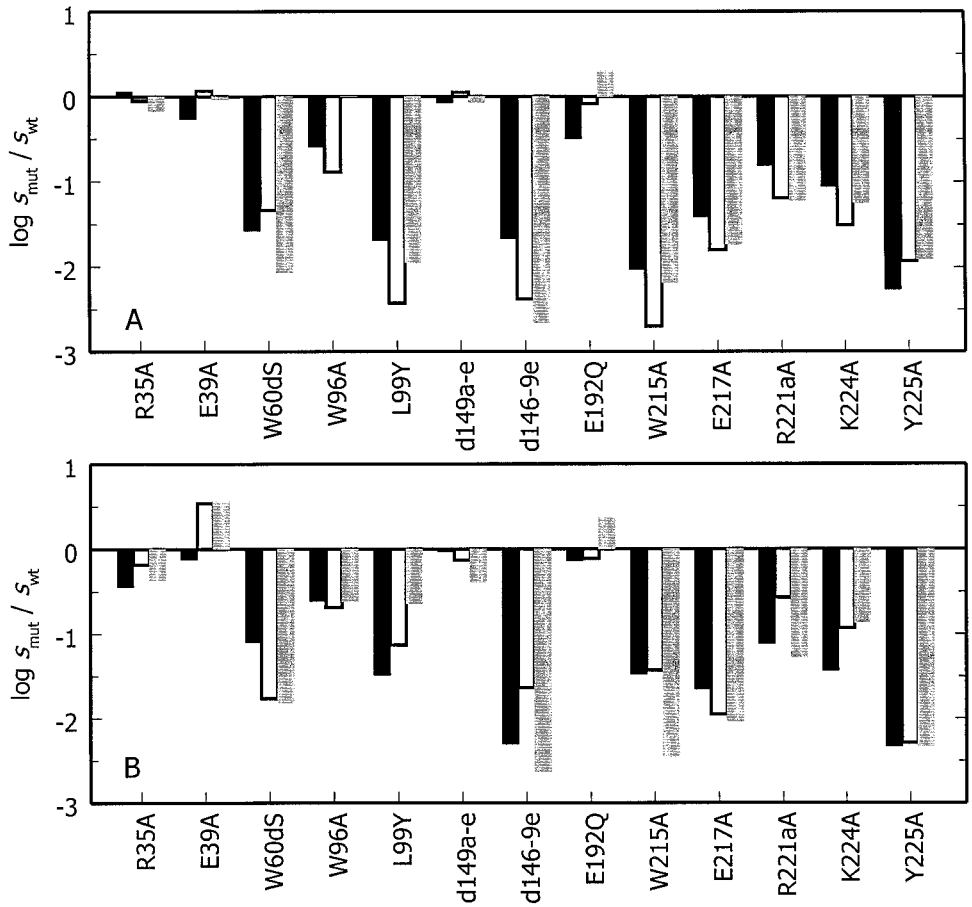

Fig. 1. Effect of site-directed mutations of thrombin residues in and around the active site (R35, E39, W60d, W96, L99, E192, W215), the Na^+ binding site (E217, R221a, K224, Y225), and the autolysis loop (E146–K149e) on the cleavage of (**A**) FPR (black bar), fibrinogen (white bar), and fibrin (gray bar), or (**B**) PAR1 (black bar), PAR3 (white bar) and PAR4 (gray bar). Numbering refers to chymotrypsin and inserted residues (e.g., R221a) are indicated by lowercase to avoid confusion with amino acid substitutions. Shown is the decimal log of the value of $s = k_{cat}/K_m$ for each mutant relative to wild-type. These values are used to color-code the epitopes for the various substrates in Figures 3 and 4. Errors are <10% of k_{cat}/K_m, or <0.04 log units. Experimental conditions are: 5 mM Tris, 0.1% PEG, 145 mM NaCl, pH 7.4, 37°C. The values of *s* for wild-type are: 97 ± 8 $\mu M^{-1}s^{-1}$ (FPR), 17 ± 1 $\mu M^{-1}s^{-1}$ (fibrinogen, FpA release), 8.1 ± 0.1 $\mu M^{-1}s^{-1}$ (fibrin, FpB release), 30 ± 1 $\mu M^{-1}s^{-1}$ (PAR1), 0.35 ± 0.02 $\mu M^{-1}s^{-1}$ (PAR3), 0.34 ± 0.01 $\mu M^{-1}s^{-1}$ (PAR4).

residues, are studied in their interaction with the PARs to identify the structural determinants of recognition. Furthermore, detailed 3D models of thrombin bound to PAR1, PAR3, and PAR4 are constructed and are consistent with the data derived from mutagenesis studies. These findings provide important new insights on how thrombin recognizes its receptors.

RESULTS

Cleavage of PAR1 showed the highest specificity among the PARs, with a value of $k_{cat}/K_m = 30 \pm 1\ \mu M^{-1}s^{-1}$ that is about 90-fold higher than the values of 0.35 ± 0.02 $\mu M^{-1}s^{-1}$ and 0.34 ± 0.01 $\mu M^{-1}s^{-1}$ determined for PAR3 and PAR4. These values are consistent with recent results obtained from the cleavage of PAR1 and PAR4 in cells.[4,10,13] The preference for PAR1 recognition is a result of lower K_m and higher k_{cat} (K_m = 7.6 ± 0.6 μM, k_{cat} = 240 ± 20 s^{-1}) compared with PAR3 (K_m = 15 ±1 μM, k_{cat} = 5.3 ± 0.5 s^{-1}) and PAR4 (K_m=120 ± 10 μM, k_{cat} = 40 ± 4 s^{-1}). Interestingly, PAR3 and PAR4 show similar specificity toward thrombin, but that results from significantly different K_m and k_{cat} values. While binding of PAR3 is preferred over PAR4, hydrolysis of PAR4 is faster than PAR3. The preference of thrombin for PAR1 is due predominantly to a faster cleavage of this receptor relative to PAR3, and a better binding relative to PAR4.

Site-Directed Mutagenesis and Epitope Mapping

The library of thrombin mutants was tested for cleavage of the PARs, fibrinogen, fibrin, and the chromogenic substrate FPR (Figs. 1 and 2). The residues replaced by Ala were chosen based on their strategic location in exosite I and around the active site that likely provide the structural determinants of PAR recognition. The role of the autolysis loop was studied with two deletion mutants that differ widely in their functional properties.[14] In those

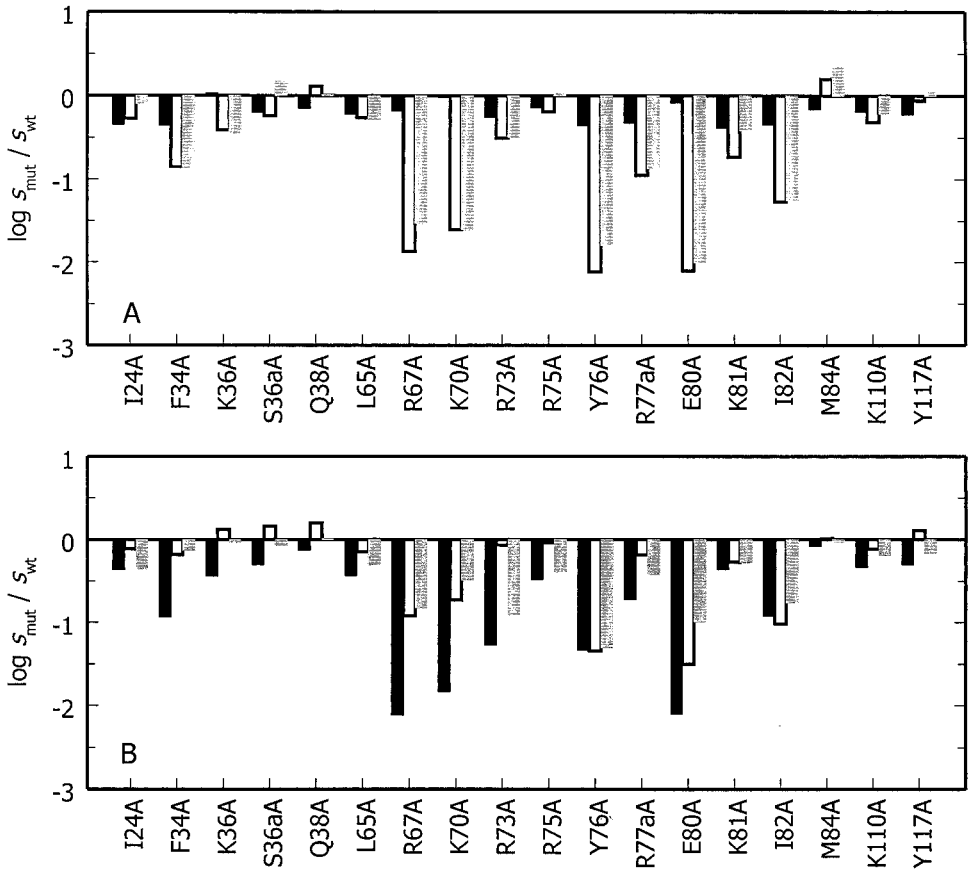

Fig. 2. Effect of site-directed mutations of thrombin residues in exosite I on the cleavage of (**A**) FPR (black bar), fibrinogen (white bar) and fibrin (gray bar), or (**B**) PAR1 (black bar), PAR3 (white bar), and PAR4 (gray bar). Shown is the decimal log of the value of $s = k_{cat}/K_m$ for each mutant relative to wild-type. These values are used to color-code the epitopes for the various substrates in Figures 3 and 4. Errors are <10% of k_{cat}/K_m, or <0.04 log units. Experimental conditions are: 5 mM Tris, 0.1% PEG, 145 mM NaCl, pH 7.4, 37°C. The values of *s* for wild-type are given in the legend to Figure 1.

cases where the values of k_{cat} and K_m could be determined separately, the effect of the mutation was mostly on the K_m (e.g., R67A–PAR1 interaction: $K_m = 400 \pm 40$ μM, $k_{cat} = 100 \pm 10$ s^{-1}; I82A–PAR3 interaction: $K_m = 290 \pm 10$ μM, $k_{cat} = 4.6 \pm 0.4$ s^{-1}), indicating that the perturbations reflected predominantly a binding defect.

Residues that affect the hydrolysis of FPR in the specificity sites S1–S4 also influence the binding of fibrinogen and the PARs (Fig. 1), pointing to an involvement of these residues in recognition of all substrates tested. This is clearly seen for Y225, which controls the architecture of the water channel around the S1 site of thrombin,[15] for W60d and L99 in the S2/S3 sites, and for W215 in the aryl binding site. The replacement of L99 with the bulkier Tyr is known to reduce the rate of diffusion of substrate into the active site.[16] The L99Y mutation displays a hierarchical effect on the cleavage of procoagulant substrates in the order fibrinogen > PAR1 > PAR4. Conversely, the mutation W60dS affects PAR4 and PAR3 more than PAR1 and the release of FpB more than FpA. Deletion of the autolysis loop involving residues 146–149 drastically affects recognition of FPR and PAR3, and it has an even greater effect on PAR1, PAR4, fibrinogen and fibrin recognition. Finally, mutation of W215 largely affects recognition of fibrinogen and PAR4.

Other residues that significantly affect FPR hydrolysis, such as E217, R221a and K224, are involved in Na^+ binding and their replacement to Ala shifts thrombin to the less active slow form.[17,18] Mutation of these residues reduces cleavage of the PARs, fibrinogen, and fibrin to an extent similar to FPR, indicating a common structural origin for the perturbation of substrate recognition. Mutation of W96 located above L99 in the S2/S3 sites has a modest effect on FPR and PAR recognition, whereas residue E192 important for thrombin interaction with protein C[19] has practically no effect on the substrates tested. Interestingly, the mutant E192Q cleaves PAR1 also downstream of the primary R41 cleavage site, specifically between the R46–N47 bond downstream of the thrombin receptor activating peptide, SFLLR.[2,3] Using a mutant of the PAR1 peptide, R41A, we obtained a value of $k_{cat}/K_m = 9.6$ $mM^{-1}s^{-1}$ for cleavage at this second site. Removal of the tethered ligand domain by cleavage at R46 or further downstream would lead to desensitization of PAR1 in cells.[20] Mutation of E39 and R35 in the primed subsites region of the active site has little effect on the

substrates tested, although a noticeable increase in the hydrolysis of PAR3 and PAR4 should be acknowledged for E39A.

The remaining residues subject to Ala replacement were all located in exosite I (Fig. 2) where they cover an extensive surface area. In no case did mutation of these residues result in compromised hydrolysis of FPR, as expected, indicating that perturbations in this region only affects macromolecular substrates like fibrinogen, fibrin, and the PARs. The effect on the PARs was in some cases significant and epitopes for each receptor could be clearly defined. In general, exosite I residues were found to be more important for binding of PAR1 than PAR3 and PAR4, and those residues involved in PAR1 recognition were also found to be involved in the binding of fibrinogen and fibrin. Residues R67, K70, and E80, and to a lesser extent R73, Y76, and I82, emerged as the most important determinants of PAR recognition in exosite I. These six residues cluster in a single spot on the surface of the molecule (Figs. 3 and 4) and are surrounded (from the top, clockwise) by K110, K81, R77a, Y117, I24, R75, F34, Q38, L65, S36a, K36, and M84 that make a small or insignificant contribution to PAR recognition. With the exception of R73, the residues important for PAR recognition (R67, K70, Y76, E80, and I82) are also important for fibrinogen and fibrin binding. R67, K70, and E80 are special insofar as they are significantly more important for recognition of PAR1 than PAR3 or PAR4. R73 is important for binding of PAR1 and PAR4, but not PAR3. On the other hand, Y76 is important for all PARs, but is even more important for fibrinogen and fibrin binding. Similar conclusions apply to I82. In no case were mutations of residues in exosite I able to discriminate between fibrinogen and fibrin, as the epitopes of these natural substrates overlap completely in this region.

3D Modeling

In order to further characterize the epitopes for PAR recognition, detailed 3D models of thrombin bound to PAR1, PAR3, and PAR4 were constructed (Fig. 3). The epitopes for FPR, fibrinogen, and fibrin recognition are shown for comparison in Figure 4. Some of the contacts involved in the recognition of each PAR are schematically represented in Figure 5. The PARs interact with thrombin in a similar manner. In addition to the ionic contact of the P1 residue with D189 at the bottom of the S1 site, the unprimed residues make important hydrophobic interactions with the W60d loop and the aryl binding site formed by L99, I174, and W215. The primed residues, on the other hand, make several ionic contacts with basic residues of exosite I (R67, R73, R77a) and hydrophobic interactions with the cluster formed by L65, Y76, and I82.

Interaction With PAR1

The surface of interaction between PAR1 and thrombin is 3450 Å^2, a value comparable to that of the thrombin–hirudin complex (3295 Å^2).[12] The thrombin–PAR1 complex shows a total of three backbone–backbone H-bonds, eight side chain–backbone or side chain–side chain H-bonds, eight ion pairs, and four clusters of more than three hydrophobic side chains. Residue L38 at P4 fills the aryl binding site formed by L99, I174, and W215. Residue D39 at P3 points to the solvent over G216 in the direction of K224 and R221a located about 9 Å away. Residue P40 at P2, F43 at P2′, and L45 at P4′ frame the W60d ring covering the catalytic residues S195 and H57. Residue R46 at P6′ loosely interacts with E39 making a solvent accessible ion pair. D50 at P9′ in PAR1 makes an ion pair interaction with R73 and is close to K149e, but makes no contact with this residue. The Nζ of K51 at P10′ makes an internal ionic contact with the carbonyl O of N49 at P8′. Y52 at P11′ stacks its ring perpendicularly to F34 and close to W141 in thrombin, thereby forming a hydrophobic cluster as in the 1NRN crystal structure.[11] E53 at P12′ makes a strong ion pair (2.2 Å) with R67 in a buried portion of exosite I, whereas in the 1NRN crystal structure the carbonyl O of E53 makes only a weak (4.6 Å) contact with the guanidinium group of R67. P54 at P13′ kinks the backbone and enables the side chains of F55 at P14′ and W56 at P15′ to penetrate a hydrophobic pocket formed by L65, I82, M84, and Y76. In the 1NRN crystal structure F55 interacts with F34 and the structure is disordered from residue W56 on. E57 at P16′ makes a solvent-accessible ion pair with R77a, whereas D58 at P17′ makes a buried ion pair with K81 and K110. Finally, K61 at P20′ makes an ion-pair with D116 and the C-terminus interacts with Nζ of K9.

Interaction With PAR3

The surface of interaction between PAR3 and thrombin is 3,200 Å^2, slightly smaller than that of the thrombin–PAR1 complex. The thrombin–PAR3 complex shows a total of four backbone–backbone H-bonds, ten side chain–backbone or side chain–side chain H-bonds, two ion pairs, and five clusters of more than three hydrophobic side chains. L35 at P4 makes a favorable hydrophobic contact with the aryl binding site, as seen for PAR1. The bigger side chain of I37 at P2, replacing the Pro at this position in PAR1, likely compensates the replacement of Arg with Lys at P1 and allows W60d to close tightly as a lid over the P1–P2 bond. The aromatic side chain of F40 of PAR3 is stacked against W60d on one side, whereas I37 contacts W60d on the opposite side. R41 at P3′ interacts with E39. The side chain of S46 at P9′ is too short to make ionic interactions with the adjacent R73, K149e or R75 in thrombin. F48 at P10′ forms a hydrophobic cluster with F34 and W141, as do F51 at P13′ and F53 at P15′ with Y76. These contacts constrain the side chains of E49 at P11′ and E50 at P12′ to point to the solvent and away from the side chains of R67, K70, R75 and R77a on the thrombin surface. The methyl groups of L56 at P18′ interact with the Cβ and Cδ of K81, and the carbonyl O of S54 at P16′ interacts with the Nζ of K81. W59 at P21′ stacks its ring perpendicularly to the ring of F114. As with PAR1, the C-terminus is ion paired with the Nζ of K9.

Interaction With PAR4

The surface of interaction between PAR4 and thrombin is 3,000 Å^2, slightly smaller than that of the thrombin–

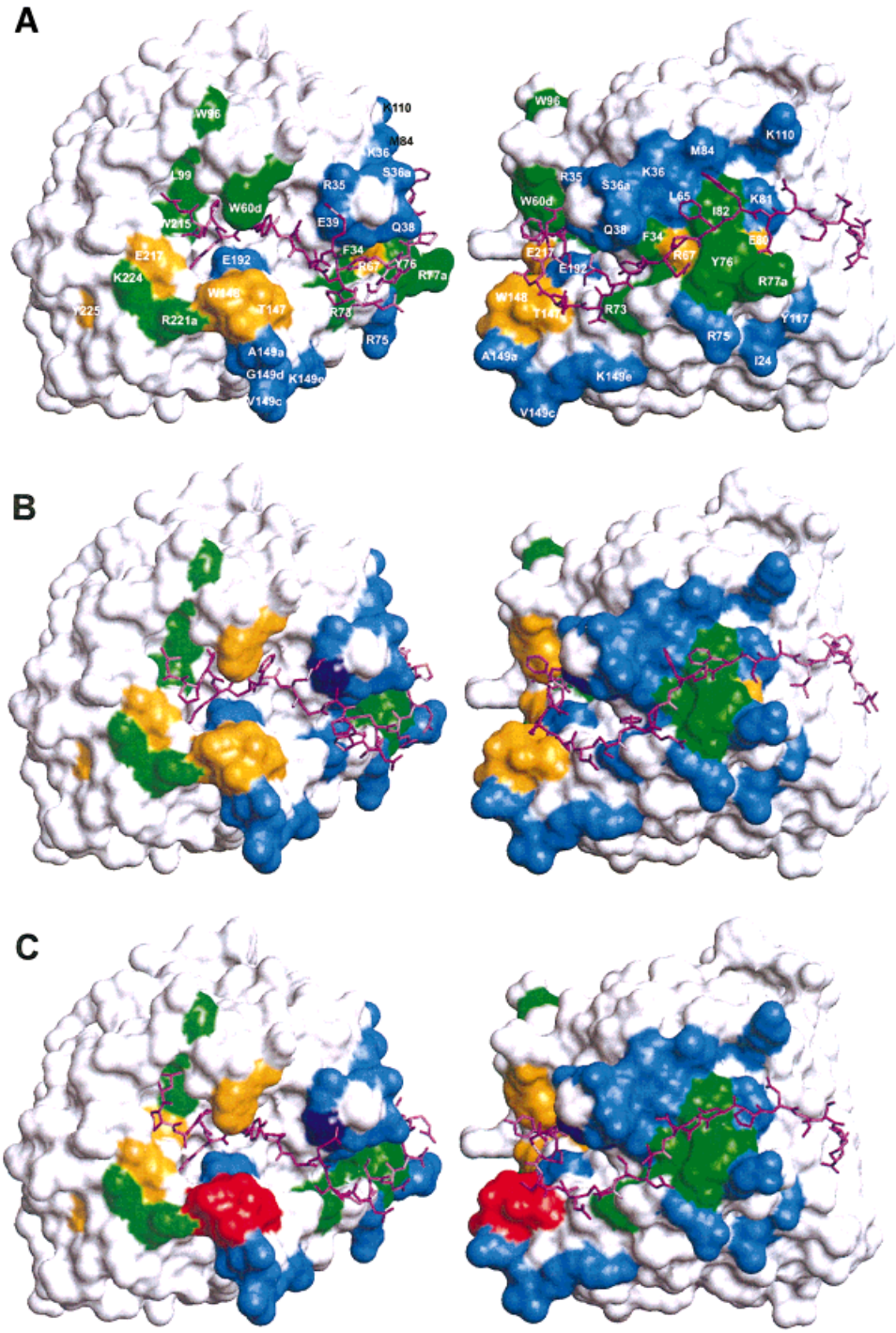

Fig. 3. Molecular mapping of the epitopes recognizing fragments of PAR1 (**A**), PAR3 (**B**), and PAR4 (C), with thrombin displayed as its solvent-accessible surface based on the coordinates 1PPB.[21] The PAR fragments are rendered as solid sticks in purple. The orientation has the active site at the center (left), or exosite I at the center (right). The residues subject to mutagenesis (labeled at the top) are color-coded based on the extent of reduction of the k_{cat}/K_m for PAR recognition (see Figs. 1 and 2) according to the scale: red ($-3.5 \div -2.5$ log units), orange ($-2.5 \div -1.5$ log units), green ($-1.5 \div -0.5$ log units), cyan ($-0.5 \div 0.5$ log units), blue ($0.5 \div 1.5$ log units). Residue K70 is buried under Y76 in exosite I and is not visible. Note the different contributions made by residues in exosite I to recognition of PAR1, PAR3, and PAR4.

PAR3 complex and more than 10% smaller than that of the thrombin–PAR1 complex. The thrombin–PAR4 complex shows a total of four backbone–backbone H-bonds, six side chain–backbone or side chain–side chain H-bonds, five ion pairs, and three clusters of more than three hydrophobic side chains. In the case of PAR4, it is L43 at P5 that makes

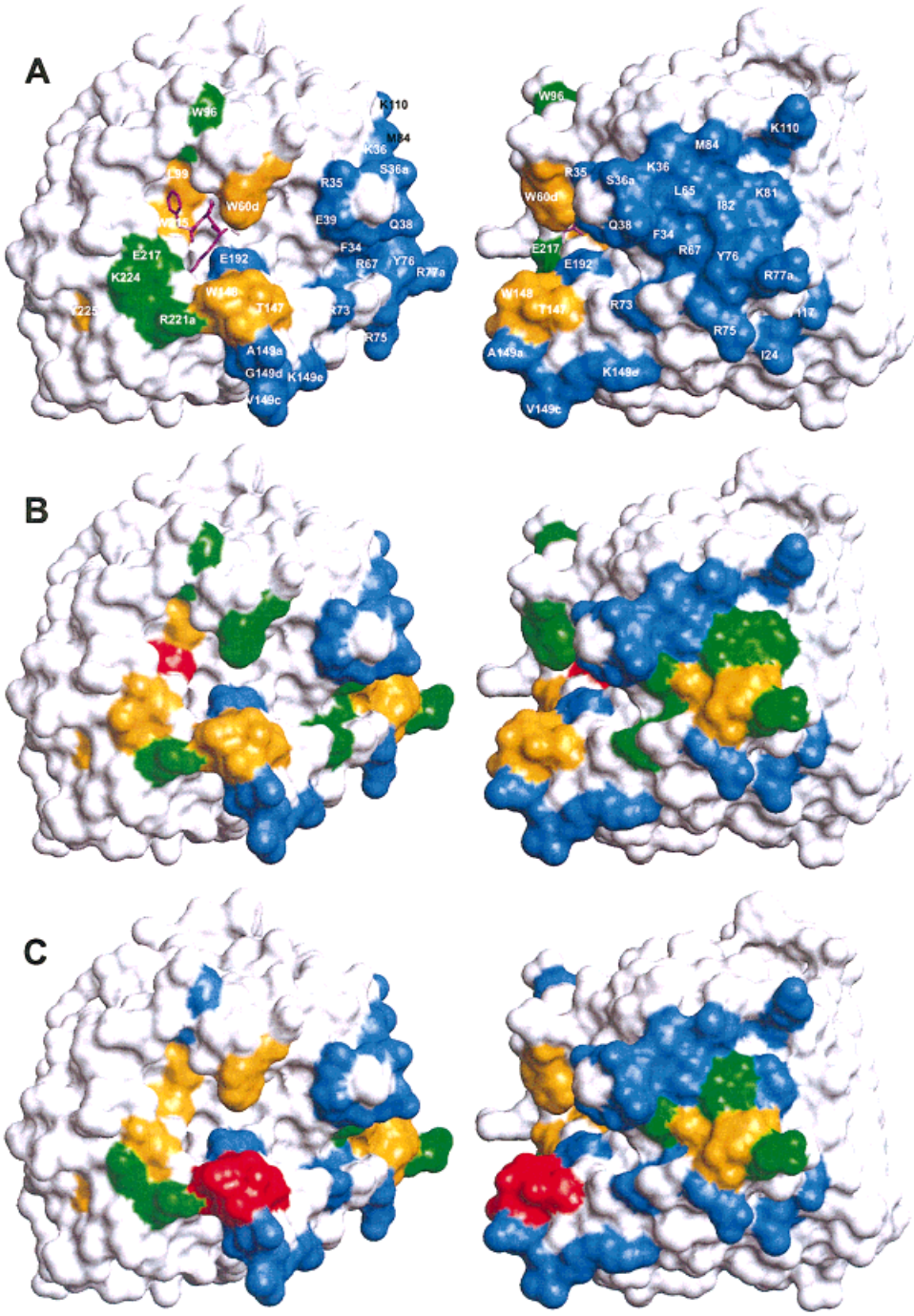

Fig. 4. Molecular mapping of the epitopes recognizing FPR (**A**), fibrinogen (**B**), and fibrin (**C**), with thrombin displayed as its solvent-accessible surface based on the coordinates 1PPB.[21] The orientation has the active site at the center (left), or exosite I at the center (right). The sequence H-D-Phe-Pro-Arg in 1PPB is displayed as solid stick in purple. The residues subject to mutagenesis (labeled at the top) are color-coded based to the extent of reduction of the k_{cat}/K_m for FPR, fibrinogen or fibrin recognition (see Figs. 1 and 2) according to the same scale as in Figure 3. Note how the contribution to FPR recognition is confined to the active site region, and how the epitopes for fibrinogen and fibrin recognition are practically identical and mirror that of PAR1 in Figure 3.

a contact with the aryl binding site due to the longer sequence separating this residue from R47 at P1. Y49 at P2 stacks its ring against W60d, whereas D57 at P10′ makes an ion pair with R73, as seen for D50 at P9′ in PAR1. L61 at P14′ and L63 at P16′ make favorable hydrophobic contacts with the cluster formed by L65, I82, and Y76. Solvent accessible ion pairs are formed by E62 at P15′ with R77a, and by R68 at P21′ with D116. On the

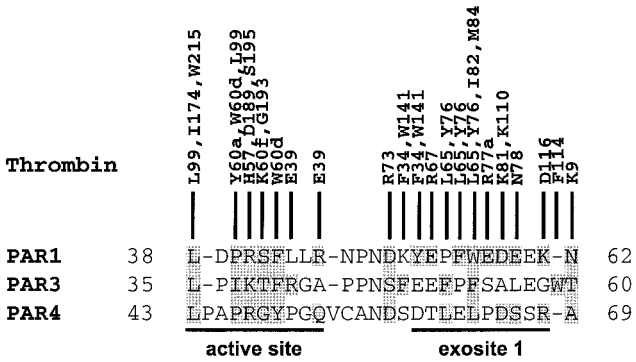

Fig. 5. Alignment of the sequences of PAR1, PAR3, and PAR4 interacting with thrombin, with some of the contacts with thrombin residues documented in the 3D models constructed in this study and shown in Figure 3. The PAR residues participating in these contacts are highlighted. Note the unique interaction of E53 of PAR1 with R67 of thrombin, which explains the higher specificity of PAR1 relative to PAR3 and PAR4 (see Fig. 2).

other hand, the ion pair between D65 at P18′ and K81 is buried. As with PAR1 and PAR3, the C-terminus is paired with the Nζ of K9.

Structure–Activity Relations

The 3D models are consistent with the mutagenesis data and help explain the role of exosite I in the recognition of the PARs. Of particular importance is the role of residues R67, K70, and E80 in preferentially affecting PAR1 recognition (Fig. 2). Mutation of these residues to Ala reduces the value of k_{cat}/K_m for cleavage of PAR1 to the values observed for PAR3 and PAR4, thereby suggesting that the interaction of E53 with R67 is a major determinant of the higher specificity (90-fold) of PAR1. According to the models, R67 makes an ionic interaction with the Oϵ2 atom of E53 of PAR1, but makes no contact with PAR3 or PAR4 (Fig. 5). Residue K70 is buried below the surface of exosite I and stabilizes the 70-loop by ion pairing with E80 and E77.[21] Mutation of K70 to Ala produces an effect similar to the mutation R67A (Fig. 2). Modeling an Ala side chain in place of K70 produces a movement of the side chain of R67 that becomes ion paired with E77. This makes the side chain of R67 unavailable for the ionic interaction with E53 of PAR1, thereby explaining the loss of specificity toward this receptor and the similarity of the effects observed between the R67A and K70A mutations. The E80A mutant shows effects similar to R67A and K70A (Fig. 2). Modeling an Ala side chain in place of E80 makes it possible for E77 to re-orient and to engage both K70 and R67 into a bi-dentate ion pair, again causing R67 to point away from E53 of PAR1. In the crystal structure 1NRN, the side chain of R67 makes a weak contact with PAR1 via the carbonyl O atom of E53, whereas the carboxylate group of E53 points to the solvent.[11] This is the result of constraints imposed on E53 by residues Y52 and F55 of PAR1 that cluster against F34 and Y76 of thrombin. Mutation of R73 affects binding of PAR1 and PAR4, but not PAR3. The guanidinium nitrogens of R73 make hydrogen bonding interactions with Oδ1 of D50 and the hydroxyl group of Y52 in PAR1, and a hydrogen bond with Oδ1 of D57 of PAR4, whereas R73 makes no such polar interactions with PAR3. I82 and Y76 affect recognition of all PARs to a similar extent. Consistent with this observation, both of these residues make hydrophobic contacts with F55 and W56 of PAR1, F51 and F53 of PAR3, and L61 and L63 of PAR4.

Other residues important for PAR recognition make contacts with the receptors in the 3D models. W60d of thrombin is framed by P40 and F43 in PAR1, I37 and F40 in PAR3, and P46 and Y49 in PAR4. W215, L99 and I174 form a binding cleft for L38 in PAR1, L35 in PAR3 and L43 in PAR4. The large perturbation due to mutation of Y225 in the Na^+ environment is mediated by changes in the architecture of the water channel embedding the S1 site.[15] Likewise, the effects of mutating E217, K224, and R221a are likely due to the loss of Na^+ binding and are allosteric in nature,[17] given that none of these residues contacts the bound receptors. Finally, the important role of the proximal sequence 146–149 of the autolysis loop remains unexplained in structural terms. As in the case of fibrinogen and fibrin,[14] this portion of the loop affects recognition of the PARs in a significant manner, but makes no contact with substrate in the crystal structure[11] or the 3D models. The effects of deleting the 146–149 sequence of the loop are probably long range and cause perturbation of the S1–S4 specificity sites, as documented by the significant loss of specificity of the deletion mutant toward the chromogenic substrate FPR.

Mapping the epitopes for the PARs according to the energetic perturbations observed in the mutagenesis studies reveal important differences in the recognition of each receptor. The most conspicuous difference is the limited importance of exosite I in PAR4 recognition. Residues important in PAR4 binding cluster around the access to the active site and involve mainly the aryl binding site (W215), the S1 site (Y225), and the proximal portion of the autolysis loop (residues 146–149). On the other hand, the primary platelet receptor PAR1 has R67 in exosite I as an important determinant of recognition, together with the adjacent residues K70, Y76, and E80. In the active site area, only Y225 in the S1 site and the proximal portion of the autolysis loop contribute to binding. In the case of PAR3, the situation is intermediate to PAR1 and PAR4. Exosite I is more important than in the case of PAR4, but less important than in the case of PAR1. The areas around E217 and W60d are more important than in the case of PAR1, but less important than for PAR4. In summary, the region around the active site including the S2–S4 sites and the proximal portion of the autolysis loop follow the hierarchy of importance in recognition PAR4 > PAR3 > PAR1, whereas exosite I follows the hierarchy PAR1 > PAR3 > PAR4. The region around the S1 site and the Na^+ site, as probed by Y225, R221a, and K224 is important for all PARs.

DISCUSSION

Previous Ala scanning mutagenesis studies of thrombin have revealed regions responsible for recognition of fibrinogen,[22] protein C,[23] and factor Va.[24] These studies have

documented an important role for residues K70 and Y76 in exosite I for fibrinogen recognition, but the most critical residues were found to be located around the Na^+ site (R221a) and the entrance to the active site (E217). Our study confirms and further refines the general trend already documented in the case of fibrinogen recognition. The new findings that emerged from our study are the almost complete overlap between the epitopes for fibrinogen and fibrin recognition, the definition of the boundaries of the epitopes of PAR1, PAR3, and PAR4, and the almost complete overlap between the epitopes for PAR1 and fibrinogen binding.

An important result from our mutagenesis study is that the region surrounding the active site and the Na^+ binding environment of thrombin is more critical for PAR recognition than exosite I. A hierarchy of effects is seen in the order PAR4 > PAR3 > PAR1 for the active site region, whereas the sequence PAR1 > PAR3 > PAR4 applies for exosite I. Of the two receptors present on human platelets, PAR1 requires the integrity of exosite I of thrombin more than PAR4, whereas PAR4 makes a significantly tighter interaction with W215 in the aryl binding site relative to PAR1. Owing to this unanticipated difference, the thrombin mutant W215A shows little activity toward PAR4, whereas it retains activity toward PAR1. On the other hand, the mutations R67A, K70A, and E80A practically abrogate the higher specificity of PAR1 relative to PAR3 and PAR4. The important role of R67, also documented in a recent mutagenesis study with the R67Q substitution,[25] can be explained at the molecular level in terms of our 3D model where R67 ion pairs with E53 of PAR1. Furthermore, the side chain of R67 becomes unavailable for this interaction when either K70 or E80 is mutated to Ala, and because of it re-orients and forms an ion pair with E77. Interestingly, the naturally occurring thrombin mutant Quick I, where R67 is mutated to Cys,[26] shows <2% activity compared to wild type in terms of fibrinogen clotting and platelet aggregation, whereas it has normal chromogenic substrate hydrolysis.[27] The properties of thrombin Quick I are consistent with the results presented in this study on the R67A mutation.

Several groups have documented the possibility of dissociating the multiple roles of thrombin in the blood. In particular, fibrinogen clotting can be dissociated from protein C activation with mutations that affect exosite I,[28] the region around the S3/S4 sites[9,18,29,30] or the Na^+ binding environment.[17] These mutations produce thrombins that function as anticoagulants both in vitro and in vivo.[29,30] We have now uncovered subtle differences in recognition of the PARs and shown that activation of PAR1 and PAR4 can be selectively compromised, although the mode of binding of these receptors to thrombin is substantially similar. The mutant W215A is 800-fold more specific for PAR1 than PAR4, whereas the mutant R67A shows the same specificity for PAR1, PAR3, and PAR4. These mutants are precious reagents for future studies of the cellular consequences of individual thrombin receptor activation in human tissues.

MATERIALS AND METHODS

Site-Directed Mutagenesis and Kinetic Studies

Site-directed mutagenesis of human α-thrombin was carried out in a HPC4-pNUT expression vector, using the Quikchange Site-directed Mutagenesis Kit from Stratagene. Expression of mutant and wild-type thrombin was carried out in baby hamster kidney cells as previously described.[15] The enzyme was activated with the prothrombinase complex for 30 min at 37°C. Some mutants required further activation with the immobilized snake venom enzyme ecarin. Activated thrombin was purified to homogeneity by FPLC using Resource Q and S columns with a linear gradient from 0.05 to 0.5 M choline chloride, 5 mM MES, pH 6 at room temperature. Mutants were checked for incomplete activation and/or autolytic digestion by N-terminal amino acid sequencing. Electrospray mass spectrometry yielded molecular weights consistent with the mutations introduced and indicated identical glycosylation between wild-type and mutant constructs. The active site concentration was determined by titration with hirudin and was found to be >95% in all cases.

All assays were carried out under experimental conditions of 5 mM Tris, 0.1% PEG, 145 mM NaCl, pH 7.4 at 37°C. The chromogenic substrate FPR was purchased from Midwest Bio-Tech. The values of k_{cat}/K_m and k_{cat} were obtained from the analysis of progress curves of the release of p-nitroaniline (measured at 405 nm) as a function of substrate concentration taking into account product inhibition, when present.

The interaction of thrombin with fibrinogen and fibrin was studied in terms of the release of FpA and FpB as described.[31] The accepted mechanism of release of fibrinopeptides states that FpA is released first from fibrinogen leading to the formation of fibrin I monomers. These monomers aggregate to form fibrin I protofibrils, from which FpB is released to give rise to fibrin II protofibrils that form the scaffold of the fibrin clot. Hence, the epitopes for fibrinogen and fibrin binding to thrombin can be mapped in a direct manner by studying the release of fibrinopeptides.

The interaction of thrombin with the PARs was studied from the kinetics of cleavage of soluble fragments corresponding to the extracellular portion of the receptors, as an extension of the strategy recently introduced for the study of thrombin–PAR1 interaction.[9] The fragments were synthesized by solid phase, purified to homogeneity by HPLC and tested for purity by mass spectrometry. The sequences of these fragments are A^{33}TNATLDPRSFLLRNPNDKYEPFWEDEEKN^{62} for PAR1, A^{31}KPTLPIKTFRGAPPNSFEEFPFSALEGWT^{60} for PAR3, and T^{39}PSILPAPRGYPGQVCANDSDTLELPDSSRA^{69} for PAR4. The intact fragments and their products of cleavage were separated by reverse phase HPLC using a C_{18} Waters Novapak column (4.6 × 250 mm, 4 μm) and a sodium phosphate buffer/acetonitrile linear gradient over 30 min, at a flow rate of 1 mL/min. Extinction coefficients for $PAR1^{33-62}$, $PAR3^{31-60}$, $PAR4^{39-69}$, and the products of cleavage were derived by calibration and quantitative amino acid analysis of highly pure standards. The identity

of products was also checked by electrospray mass spectroscopy and N-terminal amino acid sequencing. Progress curves for the hydrolysis of the PARs were generated with 3 μM substrate, whereas enzyme concentrations ranged from 0.1 nM to 100 nM depending on the activity. Reactions were stopped at different times by addition of perchloric acid to a final concentration of 0.2 M. No degradation of substrate or product fragments occurred in the absence of thrombin under all conditions tested. The concentrations of product (P) and substrate (S) for each PAR were measured as a function of time and analyzed according to the kinetic equations[9]

$$[S] = [S]_0 \exp(-se_T t) \quad (1)$$

$$[P] = [P]_\infty\{1 - \exp(-se_T t)\} \quad (2)$$

where $s = k_{cat}/K_m$ is the specificity constant for the cleavage of PAR by thrombin and e_T is the thrombin concentration. These equations are valid when the substrate concentration is below K_m. Values of K_m were obtained for wild-type and several mutant thrombins from the competitive inhibition of FPR hydrolysis by PAR1, PAR3, or PAR4 used in the concentration range 0–500 μM. These values were about 8 μM or higher in all cases. An excellent fit of the progress curves of both substrate consumption and product release was obtained for wild-type and mutant thrombins confirming the validity of equations 1 and 2.

3D-Modeling Studies

The 3D models of PAR1$^{38-62}$, PAR3$^{35-60}$, and PAR4$^{43-69}$ bound to thrombin were derived from the structures of thrombin bound to a fragment of PAR1 (1NRN, 1NRS),[11] hirudin (4HTC),[12] and hirugen (1HAH)[2] used as initial models. The PAR1, PAR3, and PAR4 sequences were threaded independently through the residues L^{38}DPR^{41} from PAR1 in 1NRS, residues G^{42}EGTPKPESH^{51} from hirudin in 4HTC, residues N^{53}GDFEEIPEEYL^{64} from hirudin in 4HTC and hirugen in 1HAH, residues D^{55}FEEIPEEY^{63} from hirugen in 1NRS, and residues Y^{52}EPFW^{56} from PAR1 in 1NRN. The sequence L^{38}DPRSFLLRNPNDK^{51} from 1NRN was discarded because the side chain of R^{41} is positioned outside the S1 pocket and the sequence S^{42}FLLRNP^{48} links the extremities of the PAR1 fragment bridging two neighbor thrombin molecules in the crystal.[11] The PAR fragments were built manually with InsightII and Biopolymer (MSI, San Diego, CA) using the existing X-ray structures (see above) as templates and substituting the desired amino acid at any given position. The side chain of Arg or Lys at the P1 position was linked through its carbonyl O to the hydroxyl O of S195 to build a covalent intermediate. Peptide chains were individually capped and H atoms were added to peptides and thrombin with Biopolymer at pH 7.0. Water molecules and the bound Na^+ as found in 1HAH were conserved as initial sets for all complexes. Water molecules were deleted only when they overlapped with a PAR residue. Different conformations were explored while keeping the backbone of thrombin frozen in its secondary structure with alternate steps of Monte-Carlo/Metropolis (dihedral space) and molecular dynamics (cartesian space) cycles of fast annealing (50–600K in 4 ps) and slow cooling (600–50K up to 20 ps). Complexes where minimized with cycles of 200 steepest descents followed by 1,500 conjugate gradients. The dielectric constant was set at 1*r, and cut-offs for non covalent bonds were set at 12 Å during Monte-Carlo and molecular dynamics and to infinity during minimization, using the force-field CFF91 and Discover (MSI). The 3D models accepted from minimization were those where the thrombin–PAR complex had an r.m.s. deviation <1.5 Å for the thrombin backbone and residues of PAR <10 Å away from thrombin. All final complexes were checked for stereochemistry with Procheck 3.0.[33] The solvent accessible surfaces of thrombin were calculated according to the Connolly algorithm and displayed as solid surface with InsightII using a probe with radius of 1.4 Å over the thrombin atoms.

REFERENCES

1. Di Cera E, Dang QD, Ayala YM. Molecular mechanisms of thrombin function. Cell Mol Life Sci 1997;53:701–730.
2. Vu TK, Hung DT, Wheaton VI, Coughlin SR. Molecular cloning of a functional thrombin receptor reveals a novel proteolytic mechanism of receptor activation. Cell 1991;64:1057–1068.
3. Vu TK, Wheaton VI, Hung DT, Charo I, Coughlin SR. Domains specifying thrombin-receptor interaction. Nature 1991;353:674–677.
4. Kahn ML, Zheng YW, Huang W, Bigornia V, Zeng D, Moff S, Farese RV, Tam C, Coughlin SR. A dual thrombin receptor system for platelet activation. Nature 1998;394:690–694.
5. Xu WF, Andersen H, Whitmore TE, Presnell SR, Yee DP, Ching A, Gilbert T, Davie EW, Foster DC. Cloning and characterization of human protease-activated receptor 4. Proc Natl Acad Sci USA 1998;95:6642–6646.
6. Nakanishi-Matsui M, Zheng YW, Sulciner DJ, Weiss EJ, Ludeman MJ, Coughlin SR. PAR3 is a cofactor for PAR4 activation by thrombin. Nature 2000;404:609–613.
7. Ishihara H, Connolly AJ, Zeng D, Kahn ML, Zheng YW, Timmons C, Tram T, Coughlin SR. Protease-activated receptor 3 is a second thrombin receptor in humans. Nature 1997;386:502–506.
8. Coughlin SR. How the protease thrombin talks to cells. Proc Natl Acad Sci USA 1999;96:11023–11027.
9. Arosio D, Ayala Y M, Di Cera E. Mutation of W215 compromises thrombin cleavage of fibrinogen, but not of PAR-1 or protein C. Biochemistry 2000;39:8095–8101.
10. Covic L, Gresser AL, Kuliopulos A. Biphasic kinetics of activation and signaling for PAR1 and PAR4 thrombin receptors in platelets. Biochemistry 2000;39:5458–5467.
11. Mathews II, Padmanabhan KP, Ganesh V, Tulinsky A, Ishii N, Chen J, Turck CW, Coughlin SR, Fenton J W. Crystallographic structures of thrombin complexed with thrombin receptor peptides: existence of expected and novel binding modes. Biochemistry 1994;33:3266–3279.
12. Rydel TJ, Tulinsky A, Bode W, Huber R. Refined structure of the hirudin-thrombin complex. J Mol Biol 1991;221:583–601.
13. Andersen H, Greenberg DL, Fujikawa K, Xu W, Chung DW, Davie EW. Protease-activated receptor 1 is the primary mediator of thrombin-stimulated platelet procoagulant activity. Proc Natl Acad Sci USA 1999;96:11189–11193.
14. Dang QD, Sabetta M, Di Cera E. Selective loss of fibrinogen clotting in a loop-less thrombin J Biol Chem 1997;272:19649–19651.
15. Guinto ER, Caccia S, Rose T, Fütterer K, Waksman G, Di Cera E. Unexpected crucial role of residue 225 in serine proteases. Proc Natl Acad Sci USA 1999;96:1852–1857.
16. Ayala YM, Di Cera E. A simple method for the determination of individual rate constants for substrate hydrolysis by serine proteases. Protein Sci 2000;9:1589–1593.
17. Dang QD, Guinto ER, Di Cera E. Rational engineering of activity

and specificity in a serine protease. Nat Biotechnol 1997;15:146–149.
18. Cantwell, AM, Di Cera E. Rational design of a potent anticoagulant thrombin J Biol Chem 2000;275: 39827–39830
19. Le Bonniec BF, Esmon CT. Glu-192→Gln substitution in thrombin mimics the catalytic switch induced by thrombomodulin. Proc Natl Acad Sci USA 1991;88:7371–7375.
20. Kuliopulos A, Covic L, Seeley SK, Sheridan PJ, Helin J, Costello CE. Plasmin desensitization of the PAR1 thrombin receptor: kinetics, sites of truncation, and implications for thrombolytic therapy. Biochemistry 1999;38:4572–4585.
21. Bode W, Turk D, Karshikov A. The refined 1.9-A X-ray crystal structure of D-Phe-Pro-Arg chloromethylketone-inhibited human alpha-thrombin: structure analysis, overall structure, electrostatic properties, detailed active-site geometry, and structure-function relationships. Protein Sci 1992;1:426–471.
22. Tsiang M, Jain AK, Dunn KE, Rojas ME, Leung LLK, Gibbs CS. Functional mapping of the surface residues of human thrombin. J Biol Chem 1995;270;16854–16863.
23. Hall SW, Nagashima M, Zhao L, Morser J, Leung LLK. Thrombin interacts with thrombomodulin, protein C, and thrombin-activatable fibrinolysis inhibitor via specific and distinct domains. J Biol Chem 1999;274;25510–25516.
24. Myles T, Yun TH, Hall SW, Leung LL. An extensive interaction interface between thrombin and factor V is required for factor V activation. J Biol Chem 2001;276:25143–25149.
25. Myles T, Le Bonniec BF, Stone SR. The dual role of thrombin's anion-binding exosite-I in the recognition and cleavage of the protease-activated receptor 1. Eur J Biochem 2001;268:70–77.
26. Henriksen RA, Mann KG. Identification of the primary structural defect in the dysthrombin thrombin Quick I: substitution of cysteine for arginine-382. Biochemistry 1988;27:9160–9165.
27. Henriksen RA, Owen WG. Characterization of the catalytic defect in the dysthrombin, Thrombin Quick. J Biol Chem 1987;262:4664–4669.
28. Wu Q, Sheehan JP, Tsiang M, Lentz SR, Birktoft JJ, Sadler, JE. Single amino acid substitutions dissociate fibrinogen-clotting and thrombomodulin-binding activities of human thrombin. Proc Natl Acad Sci USA 1991;88:6775–6779.
29. Gibbs CS, Coutre SE, Tsiang M, Li WX, Jain AK, Dunn KE, Law VS, Mao CT, Matsumura SY, Mejza SJ, Paborsky LR, Leung LL. Conversion of thrombin into an anticoagulant by protein engineering. Nature 1995;378:413–416.
30. Di Cera E. Anticoagulant Thrombins. Trends Cardiovasc Med 1998;8:340–350.
31. Vindigni A, Di Cera E. Release of fibrinopeptides by the slow and fast forms of thrombin. Biochemistry 1996;35:4417–4426.
32. Vijayalakshmi J, Padmanabhan KP, Mann KG, Tulinsky A. The isomorphous structures of prethrombin2, hirugen-, and PPACK-thrombin: changes accompanying activation and exosite binding to thrombin. Protein Sci 1994;3:2254–2271.
33. Laskowski RA, Moss DS, Thornton JM. Main-chain bond lengths and bond angles in protein structures. J Mol Biol 1993;231:1049–1067.